

The magnetic structure of $(\text{Fe}_{30-x}\text{Ru}_x)\text{B}_{20}$ metallic glasses

This article has been downloaded from IOPscience. Please scroll down to see the full text article.

1998 J. Phys.: Condens. Matter 10 2617

(<http://iopscience.iop.org/0953-8984/10/12/006>)

View [the table of contents for this issue](#), or go to the [journal homepage](#) for more

Download details:

IP Address: 171.66.16.151

The article was downloaded on 12/05/2010 at 23:20

Please note that [terms and conditions apply](#).

The magnetic structure of $(\text{Fe}_{80-x}\text{Ru}_x)\text{B}_{20}$ metallic glasses

A R Wildes[†], R A Cowley[†], S Al-Heniti[‡], N Cowlam[‡], J Kulda[§] and E Lelièvre-Berna[§]

[†] Clarendon Laboratory, University of Oxford, Parks Road, Oxford, UK

[‡] Department of Physics, University of Sheffield, Sheffield S3 7RH, UK

[§] Institut Laue–Langevin, BP 156, 38042 Grenoble Cédex 9, France

Received 16 July 1997, in final form 3 November 1997

Abstract. Neutron scattering with polarization analysis has been used to examine the spin-dependent absolute neutron cross-section of $\text{Fe}_{80}\text{B}_{20}$, $\text{Fe}_{70}\text{Ru}_{10}\text{B}_{20}$ and $\text{Fe}_{62}\text{Ru}_{18}\text{B}_{20}$ metallic glasses. $\text{Fe}_{80}\text{B}_{20}$ is shown to be a canted ferromagnet with an average canting angle of approximately 49° in a field of 2 T. Contrary to expectations, there is little or no canting in the samples containing ruthenium as proved by the absence of spin-flip scattering. The magnetic structure of $\text{Fe}_{62}\text{Ru}_{18}\text{B}_{20}$ has been studied as a function of temperature and magnetic field history. When cooled to 4.2 K in zero field the observed scattering is not consistent with the presence of a spin-glass phase. An increase in the projection of the moments in the direction of the applied field was observed when the sample was cooled to 4.2 K in an applied field of 2 T. The results are discussed in the context of current structural models of $(\text{Fe}_{80-x}\text{Ru}_x)\text{B}_{20}$ glasses.

1. Introduction

The question of whether there is canting of the moments in ferromagnetic iron based metallic glasses has been discussed for some years amongst both theorists and experimentalists. A large part of the argument has dwelt on whether the variation of magnetic moment per atom with composition in these systems is due to canting of the moments away from a collinear arrangement, or whether there are changes in the magnitude of the moment itself from atom to atom. Some answers to this question have been found in recent years, in particular on samples of $\text{Fe}_{80-x}\text{B}_{20+x}$ glasses.

The most direct method for investigating the microscopic arrangement of the magnetic moments in a system is to use neutron diffraction with polarization analysis. Such a measurement was used by Cowley *et al* (1991) on $\text{Fe}_{83}\text{B}_{17}$, who discovered evidence for considerable canting away from a collinear ferromagnetic structure. This finding has been corroborated using Mössbauer measurements on similar samples (Harker and Pollard 1989), and from detailed magnetization measurements (Kaul and Babu 1994), although the results do not agree on the degree of the canting.

Previous theoretical work (Krompiewski *et al* 1989, Hafner *et al* 1994) has modelled these structures using a collinear ferromagnetic model. However, Liebs and Fähnle (1996) have recently published a calculation of the spin configurations on $(\text{Fe}_x\text{Ni}_{1-x})_{80}\text{B}_{20}$ as a function of mass density, using an *ab initio* band structure model without the constraint of collinearity. They showed that, at a mass density of 7.44 g cm^{-3} , the most energetically favourable state in $\text{Fe}_{80}\text{B}_{20}$ has spins deviating by a mean angle of $58 \pm 45^\circ$ from the applied field direction. For a mass density of 7.08 g cm^{-3} the most energetically favourable

state is collinear and ferromagnetic; however an energy increase of between 1 and 4 meV per transition metal atom produces a canting of between 20 and 50° from the applied field direction. They concluded that there may be low-energy states that have appreciable canting at this mass density.

The introduction of a second transition metal into iron–boron metallic glasses changes the magnetic properties of the system. The work by Liebs and Fähnle (1996) has included a model of the spin distributions in $\text{Fe}_{40}\text{Ni}_{40}\text{B}_{20}$, and their work suggests that the lowest-energy state in this system is collinear. This is in contradiction to the experimental results of Cowley *et al* (1991), which suggests that the (FeNi)B system is not yet fully understood.

It has been proposed that the addition of ruthenium increases the degree of canting. Paulose *et al* (1986, 1987, 1988) have carried out ac susceptibility, dc magnetization and Mössbauer measurements on $\text{Fe}_{80-x}\text{Ru}_x\text{B}_{20}$ metallic glasses. As a result they suggest that $\text{Fe}_{62}\text{Ru}_{18}\text{B}_{20}$ is a re-entrant spin glass below 70 K and has appreciable canting. The aim of the present work was to use neutron diffraction with polarization analysis of the scattered beam for both spin-states of the incident beam to measure the amount of canting on a selection of $\text{Fe}_{80-x}\text{Ru}_x\text{B}_{20}$ samples.

2. The samples

Three metallic alloy glass samples with compositions $\text{Fe}_{80}\text{B}_{20}$, $\text{Fe}_{70}\text{Ru}_{10}\text{B}_{20}$ and $\text{Fe}_{20}\text{Ru}_{18}\text{B}_{20}$ were prepared for this study. Parent ingots were made by argon-arc melting of spectroscopically pure constituents with negligible weight loss. Natural boron was used because of technical difficulties with the ^{11}B isotope available. The metallic glass ribbon was produced by conventional chill-block melt-spinning, using a steel wheel with a rim speed of approximately 50 m s⁻¹. The melt spinning was performed under a helium atmosphere. The resulting ribbon, which was ≈ 25 μm thick and ≈ 1 mm wide, was wound onto a flat plate for x-ray measurements, which were made on a Philips PW 1050 vertical goniometer with a curved crystal monochromator and Mo $K\alpha$ radiation $\lambda = 0.711$ Å. The scattering from both sample and background was measured over a range of scattering angles $5^\circ < 2\theta < 160^\circ$, with each measurement taking approximately 18 h. Figure 1 shows the structure factors $S(Q)$ (Q is the scattering vector $Q = 4\pi \sin\theta/\lambda$) obtained for the three glasses from the corrected and normalized diffraction data. The characteristic form of these $S(Q)$ and presence of the four diffuse maxima confirm that the three samples are genuine metallic glasses. The reduced radial distribution function $G(r) = 4\pi r(\rho(r) - \rho_0)$ was obtained for each glass by the usual Fourier transform and the three curves are shown in figure 2. They are plotted out to a value of radial distance $r = 16$ Å, which corresponds to a ‘range of structural variations’ $r_s = 2\pi/\Delta Q$, where ΔQ is the width of the first maximum in $S(Q)$; here $\Delta Q \approx 0.4$ Å⁻¹ for all three samples. The $G(r)$ curves all show a well developed first-neighbour peak and a second peak with the characteristic shoulder. The first-neighbour distances for these glasses lie between $2.50 < r_1 < 2.54$ Å as the proportion of ruthenium increases and the coordination number remains sensibly constant at around $n_1 \approx 12.5$. The conclusion that the addition of ruthenium (whose Goldschmidt diameter is larger than that of iron by only 5%) does not significantly change the glassy structure has also been confirmed by a second series of x-ray measurements on a range of seven samples with the composition $\text{Fe}_{83-x}\text{Ru}_x\text{B}_{17}$ with $0 < x < 22$ (Al-Heniti and Cowlam, to be published). Neutron small-angle scattering (SAS) measurements have also recently been made on the LOQ instrument at the ISIS neutron source, Rutherford Appleton Laboratories, on both FeRuB and FeZr metallic glasses and are currently being analysed. A

comparison has been made between glassy samples whose x-ray diffraction patterns contain no Bragg peaks and other samples prepared under less optimized conditions which have small crystalline contamination. It was found that the FeRuB specimens used in this present work have very small SAS intensities and are essentially homogeneous. Details of these structural studies will be presented elsewhere (Al-Heniti and Cowlam, to be published). Magnetization measurements to check that these samples are indeed similar to those of Paulose *et al* (1986, 1987, 1988) are also currently in progress, and the preliminary data suggest that this is indeed the case.

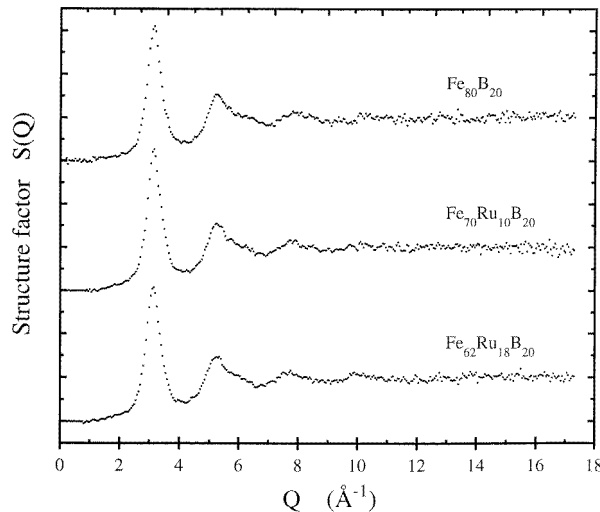


Figure 1. The total structure factors $S(Q)$ against Q for the three metallic glasses $Fe_{70}Ru_{10}B_{20}$ and $Fe_{62}Ru_{18}B_{20}$ obtained with x-rays.

Approximately 3.5, 6.2 and 6.3 g of $Fe_{80}B_{20}$, $Fe_{70}Ru_{10}B_{20}$ and $Fe_{62}Ru_{18}B_{20}$ ribbon respectively was wound onto a flat steel and brass former of a kind described previously (Cowley *et al* 1991) to make planar samples for the neutron scattering experiments. The mass densities of these samples were calculated to be 6.80, 7.21 and 7.56 g cm⁻³ respectively. However, the atomic number densities *decrease* with increasing percentage of ruthenium, as the atomic weight of the samples changes rapidly with the addition of the heavier element.

3. The neutron scattering experiment

The neutron scattering experiments were carried out using the IN20 triple-axis spectrometer at the Institut Laue-Langevin. The instrument was configured to measure the four polarization state cross-sections using Heusler alloy crystals as polarizing monochromator and analyser. The samples were mounted in a superconducting cryomagnet capable of cooling to temperatures below 2 K in magnetic fields up to 6 T. The cryomagnet was accurate to better than ± 0.1 K in temperature, and stable to $\pm 1\%$ in magnetic field. The field and hence the neutron polarization was perpendicular to the scattering plane. The orientation of the neutron spins just before and just after the sample was then controlled by spin flippers. Only the elastic cross-sections were measured, with the magnitudes of the incident and scattered wavevectors being 4.1 \AA^{-1} . Horizontal collimators of $60'$ were put

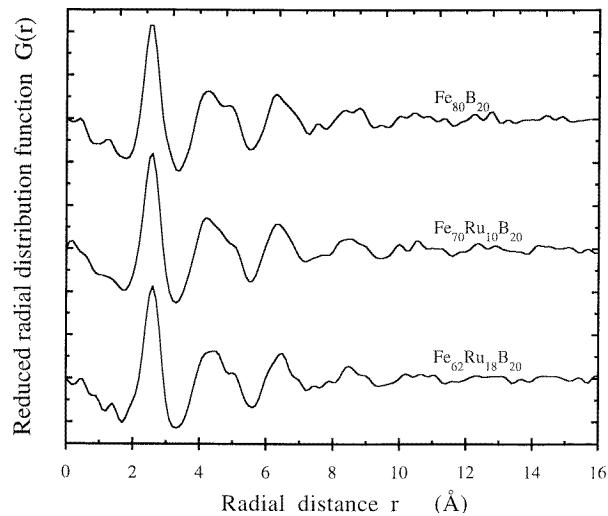


Figure 2. Radial distribution features, $G(r)$, which were obtained from the Fourier transform of the structure factors in figure 1, are given for the three metallic glasses $\text{Fe}_{80}\text{B}_{20}$, $\text{Fe}_{70}\text{Ru}_{10}\text{B}_{20}$ and $\text{Fe}_{62}\text{Ru}_{18}\text{B}_{20}$.

in the monochromator-sample and sample-analyser positions. In this configuration and at $Q = 3.1 \text{ \AA}^{-1}$, the wavevector resolution is $2.7 \times 10^{-2} \text{ \AA}^{-1}$ (FWHM) along the scattering vector, while the energy resolution at zero energy transfer is 3.0 meV (FWHM).

A field high enough to saturate the samples was chosen in order to avoid depolarization effects due to magnetic domains. Previous DC magnetization studies of $\text{Fe}_{80-x}\text{Ru}_x\text{B}_{20}$ (Paulose *et al* 1987) have shown that, for $x < 18$, the magnetization increases sharply with field up to approximately 0.1 T and then saturates to become almost constant with increasing field. It was therefore assumed that a magnetic field of 2 T would polarize all the samples used in the experiment. 2 T was used because larger fields than this create fringing fields that interfere with the spin-flippers. It should be noted here that Paulose *et al* (1987) concluded that a field of 8 T is insufficient for the moments in the sample to become collinear and thus considerable canting effects were expected at 2 T.

The four polarization-state cross-sections for the $\text{Fe}_{80}\text{B}_{20}$ and $\text{Fe}_{70}\text{Ru}_{10}\text{B}_{20}$ samples were measured at a temperature of 4.2 K, and three sets of measurements of the four cross-sections were carried out for the sample of $\text{Fe}_{62}\text{Ru}_{18}\text{B}_{20}$. This sample is reported to have a re-entrant spin-glass structure, with a Curie temperature of approximately 200 K and a spin-glass transition at approximately 60 K (Paulose *et al* 1988). Two measurements were then carried out at 4.2 K; one in which the sample was cooled from room temperature in zero field; and one in which the sample was cooled in 2 T. In both cases, the measurement was carried out with the sample in a field of 2 T. It was expected that when the sample was cooled in the field, a preferred magnetization direction would be 'frozen in', and that there would be a significant difference between this measurement and the measurement when the sample was cooled in zero field. The third measurement on $\text{Fe}_{62}\text{Ru}_{18}\text{B}_{20}$ was conducted at 100 K. The sample was cooled in a constant field of 2 T for this measurement; however, at 100 K the sample was expected to be ferromagnetic (Paulose *et al* 1988) and therefore its magnetic behaviour is independent of its field history.

The scattering was measured for a range of momentum transfers $1 \leq Q \leq 6.3 \text{ \AA}^{-1}$,

and with the sample in transmission geometry. The scattering vector lay in the plane of the sample, and thus the sample was rotated along with the detector in a $(\theta, 2\theta)$ arrangement. Geometric corrections to obtain the cross-sections were then made.

In order to calculate the absolute cross-sections from these samples, a number of other measurements were made. The scattering was measured through an indium 'blank' held in the same sample former as used for the metallic glasses, over the same range of scattering vectors. Indium is close to a perfect absorber, with a large absorption cross-section (193.8 barn/atom) and a small incoherent scattering cross-section (0.54 barn/atom). Thus, by matching the attenuation of the indium to that of a sample, a very good measure of the true background for the measurement could be determined and subtracted from the measured spectra.

The second measurement used a vanadium sample. Vanadium has a large incoherent cross-section (5.08 barn/atom) and a small coherent cross-section (0.01838 barn/atom), which makes it a very good calibration standard for neutron scattering. Factors accounting for resolution and other instrumental effects were determined from the scattered intensity from the vanadium and these factors were then applied to the scattered intensity from the sample. In addition, the vanadium provided a reference from which the absolute cross-sections could be calculated, because the vanadium scattering is incoherent with a magnitude of $5.08/4\pi = 0.404$ barn $\text{sr}^{-1}/\text{atom}$.

Finally, the efficiencies of the polarizing elements were determined. In theory these can also be extracted from the scattering from vanadium, as in the absence of magnetic, isotropic and coherent scattering one-third of the single-scattering events are non-spin-flip and the other two-thirds spin-flip. In practice however, the errors on the data points make it very difficult to extract meaningful values. Thus, the efficiencies were estimated by measuring the flipping ratios of the main beam without a sample in the beam. The equations of Cowley *et al* (1991) were adapted, with p_1 being the percentage of the beam not polarized after diffraction from the monochromator, p_2 being a similar quantity after diffraction from the analyser, and with p_3 and p_4 describing the depolarization due to the flippers before and after the sample respectively. The values of the polarization parameters obtained were $p_1 = p_2 = 0.031 \pm 0.004$, $p_3 = 0.021 \pm 0.009$ and $p_4 = 0.019 \pm 0.009$.

A correction for absorption was made by integrating over all path lengths in the samples. Multiple-scattering corrections made using the methods described by Sears (1975) and by Harders *et al* (1985).

Each step of the data analysis is independent of the others, and consequently the calculated errors in each step of the data analysis is also independent. The final error of the analysed data points was therefore calculated in the standard way of addition of the errors in quadrature, each error weighted by the partial derivative of the analysis function with respect to the variable that contained the error.

4. Neutron scattering theory

Neutron scattering with polarization analysis was extensively described by Moon *et al* (1969) and by Lovesey (1984). Cowley *et al* (1991) carried out a very similar experiment to the present one and included a discussion of the expected partial cross-sections. As this experiment extended the technique to obtain the absolute cross-sections, some further discussion is needed.

Unlike the measurements on $Fe_{83}B_{17}$, natural boron was used to make the samples used in this experiment and consequently incoherent scattering could not be ignored. Thus, extending the equations given by Cowley *et al* (1991) the partial cross-sections for the

different spin configurations in the present experiment are:

$$\begin{aligned}
 \frac{d\sigma^{++}}{d\Omega} &= \frac{d\sigma_{nc}}{d\Omega} + \frac{d\sigma_{ii}}{d\Omega} + \frac{1}{3} \frac{d\sigma_{nsi}}{d\Omega} \\
 &\quad + \left\langle \left| \sum_{lm} (d_l d_m^* S_{zl} S_{zm}^* + b_l d_m^* S_{zm}^* + b_m^* d_l^* S_{zl}) \exp(i\mathbf{Q} \cdot (\mathbf{R}_l - \mathbf{R}_m)) \right| \right\rangle \\
 \frac{d\sigma^{--}}{d\Omega} &= \frac{d\sigma_{nc}}{d\Omega} + \frac{d\sigma_{ii}}{d\Omega} + \frac{1}{3} \frac{d\sigma_{nsi}}{d\Omega} \\
 &\quad + \left\langle \left| \sum_{lm} (d_l d_m^* S_{zl} S_{zm}^* - b_l d_m^* S_{zm}^* - b_m^* d_l^* S_{zl}) \exp(i\mathbf{Q} \cdot (\mathbf{R}_l - \mathbf{R}_m)) \right| \right\rangle \\
 \frac{d\sigma^{+-}}{d\Omega} &= \frac{d\sigma^{-+}}{d\Omega} = \frac{2}{3} \frac{d\sigma_{nsi}}{d\Omega} + \left\langle \left| \sum_{lm} d_l d_m^* S_{xl} S_{xm}^* \exp(i\mathbf{Q} \cdot (\mathbf{R}_l - \mathbf{R}_m)) \right| \right\rangle
 \end{aligned} \tag{1}$$

where $d\sigma_{nc}/d\Omega$ is the coherent part of the nuclear differential cross-section, $d\sigma_{ii}/d\Omega$ is the isotropic incoherent differential cross-section and $d\sigma_{nsi}/d\Omega$ is the nuclear spin incoherent differential cross-section. $d_l = (\gamma e^2/2mc^2)g_l f_l(\mathbf{Q})$, where $f_l(\mathbf{Q})$ is the magnetic form factor. The z and x directions are respectively perpendicular to the scattering plane and perpendicular to both \mathbf{Q} and z . The incoherent contributions to the partial cross-sections can be calculated from tables of Sears (1992). Throughout the rest of this paper the partial differential cross-sections $d\sigma^{++}/d\Omega$ and $d\sigma^{--}/d\Omega$ will be referred to as the non-spin-flip cross-sections and the partial differential cross-sections $d\sigma^{+-}/d\Omega$ and $d\sigma^{-+}/d\Omega$ as the spin-flip cross-sections. Thus, equations (1) show that when the field and polarization directions are along the z direction, the spin-flip cross-sections give the component of moments along x ; and the non-spin-flip cross-sections give the nuclear coherent scattering, the magnetic coherent scattering in the field direction and nuclear–magnetic cross terms.

5. Results and discussion

5.1. Magnetic structure as a function of composition

Figures 3 to 5 show the spin-flip and non-spin-flip cross-sections obtained for the $\text{Fe}_{80-x}\text{Ru}_x\text{B}_{20}$ metallic glasses measured at 4.2 K. As expected, the two spin-flip cross-sections $d\sigma^{+-}/d\Omega$ and $d\sigma^{-+}/d\Omega$ were equivalent to within the error bars and therefore in all the analysis the results were averaged.

There are three reasons to assume that the normalization of the data has been done correctly. The first is that all the normalized values are, within error, greater than or equal to the corresponding calculated incoherent cross-sections. The second is that the total scattering for any amorphous sample should converge to the coherent nuclear cross-section plus incoherent contributions at large Q . Neglecting incoherent contributions, for a binary system with no correlation between nuclei this is given by $cb_1^2 + (1-c)b_2^2$ barn $\text{sr}^{-1}/\text{atom}$ where b_1 , b_2 are the scattering lengths of elements 1 and 2 and c is the concentration of element 1. Equations (1) show that the full magnitude of this cross-section will be seen in both non-spin-flip cross-sections. The value of this cross-section plus the incoherent contributions for $\text{Fe}_{80}\text{B}_{20}$ is 0.81 barn $\text{sr}^{-1}/\text{atom}$ and slightly less for the samples containing ruthenium. While the measurements here were not made to a value of Q high enough for the non-spin-flip cross-sections to converge, it can be seen that in all cases the magnitude of the non-spin-flip scattering at about 6 \AA^{-1} compares well with the above value. The third reason is a comparison with earlier results, which will be discussed below.

Figures 3 show the results for $\text{Fe}_{80}\text{B}_{20}$. This sample is very similar in composition to the $\text{Fe}_{83}\text{B}_{17}$ sample examined by Cowley *et al* (1991), and the shape and the magnitudes of

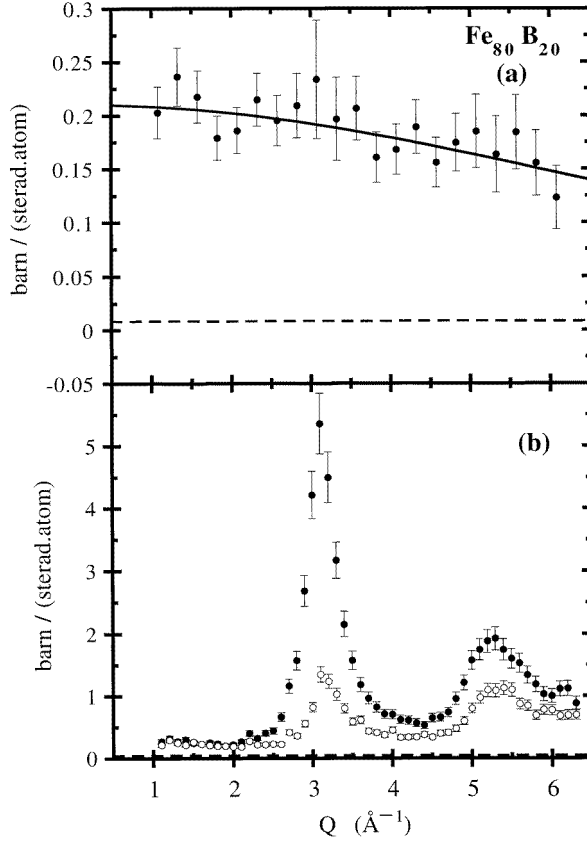


Figure 3. The spin-flip (a) and non-spin-flip (b) cross-sections from $Fe_{80}B_{20}$ measured at 4.2 K. Figure 3(a) shows the average $\frac{1}{2}(\frac{d\sigma^{+-}}{d\Omega} + \frac{d\sigma^{-+}}{d\Omega})$. Figure 3(b) shows the two non-spin-flip cross-sections, $\frac{d\sigma^{++}}{d\Omega}$ (●) and $\frac{d\sigma^{--}}{d\Omega}$ (○). The dotted line in figure 3(a) is $\frac{2}{3}d\sigma_{nsi}/d\Omega$. The dotted line in figure 3(b) is the value of $d\sigma_{ii}/d\Omega + \frac{1}{3}d\sigma_{nsi}/d\Omega$. $d\sigma_{ii}/d\Omega$ is the isotropic incoherent cross-section and $d\sigma_{nsi}/d\Omega$ is the nuclear spin incoherent cross-section. All incoherent cross-sections are calculated using the values from Sears (1992). The solid line in figure 3(a) is the fit to equation (2).

both the spin-flip and non-spin-flip scattering are similar. The maximum of $\frac{d\sigma^{++}}{d\Omega}$ for $Fe_{80}B_{20}$ is $5.4 \text{ barn sr}^{-1}/\text{atom}$ after accounting for the incoherent scattering, in comparison to the normalized value of $4.7 \text{ barn sr}^{-1}/\text{atom}$ obtained for $Fe_{83}B_{17}$ using a different method (Cowley *et al* 1991). The spin-flip scattering is $0.19 \pm 0.02 \text{ barn sr}^{-1}/\text{atom}$ for $Q = 1.075 \text{ \AA}^{-1}$ for $Fe_{80}B_{20}$, which is larger than the value of approximately 0.1 for $Fe_{83}B_{17}$ with $Q \approx 1.075 \text{ \AA}^{-1}$ (Cowley *et al* 1991).

An equation for the form factor of Fe^{3+} can be fitted to the spin-flip data for $Fe_{80}B_{20}$. An analytic approximation for the normalized form factor is

$$f(Q) = \sum_{i=1}^3 A_i \exp\left(\frac{-B_i W Q^2}{16\pi^2}\right) + C \quad (2)$$

and the parameters A_i , B_i and C are given by Brown (1995). The form factor is normalized so that $f(0) = 1$, and the values of the parameters for Fe^{3+} are given in table 1. Cowley *et al* (1991) followed the example of Bletry and Sadoc (1975) by introducing the parameter

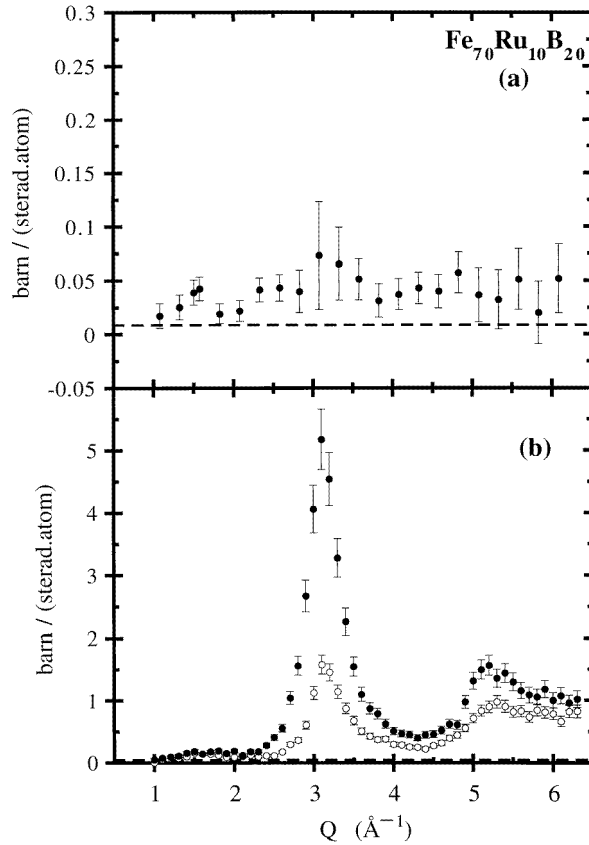


Figure 4. Spin-flip (a) and non-spin-flip (b) cross-sections from $\text{Fe}_{70}\text{Ru}_{10}\text{B}_{20}$ at 4.2 K. The format and definitions are the same as for figure 3.

W to account for the broadening of the form factor in an amorphous sample and obtained $W = 0.35$. This was different from the value obtained by Guoan *et al* (1982) of $W = 0.8$. A fit of the form-factor squared to the spin-flip scattering from $\text{Fe}_{80}\text{B}_{20}$, shown in figure 3(a), gives a value of $W = 0.10 \pm 0.04$, considerably smaller than both the earlier results.

Table 1. Parameters to calculate the analytic expression for the form factor of Fe^{3+} .

i	A_i	B_i	C
1	0.3972	13.244	
2	0.6295	4.903	0.0044
3	-0.0314	0.350	

The fit also gives the magnitude of the cross-section for $Q = 0$, which can be used in a simple model to estimate to the projection of the moments in the x direction. If as an approximation it is assumed the moments are randomly canted on a cone, the magnitude of the cross-section is given by $\frac{1}{2}(\gamma e^2/2mc^2)^2 \langle S_x^2 \rangle = 0.036 \langle S_x^2 \rangle$ barn $\text{sr}^{-1}/\text{atom}$. The fitted function has a magnitude of 0.20 ± 0.01 , from which the value for $\langle S_x^2 \rangle^{\frac{1}{2}} = 2.3 \pm 0.3 \mu_B$ is

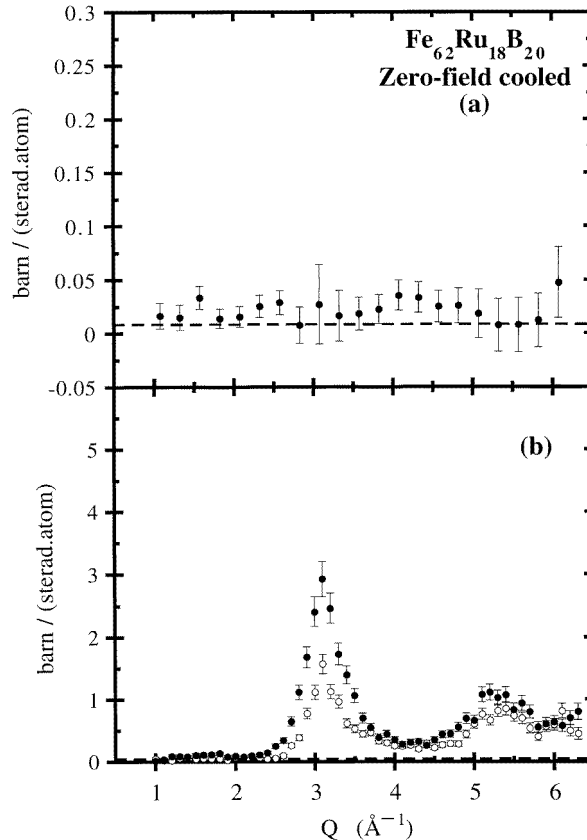


Figure 5. Spin-flip (a) and non-spin-flip (b) cross-sections from $Fe_{62}Ru_{18}B_{20}$ at 4.2 K, the sample cooled in zero field. The format and definitions are the same as for figure 3.

obtained. DC magnetization measurements in a field of 8 kOe and at a temperature of 4.2 K give an Fe moment of approximately $2 \mu_B$ in $Fe_{80}B_{20}$ (Paulose *et al* 1988). If this is taken to be the magnitude of the component of the moments parallel to the magnetic field, then the moments are canted on average from the field direction by $49 \pm 6^\circ$. This is intermediate between the measured result of $30 \pm 6^\circ$ obtained for $Fe_{83}B_{17}$ and the theoretical result of $58 \pm 45^\circ$ of Liebs and Föhnle (1996).

A possible explanation for the differences in the experimental results for $Fe_{80}B_{20}$ and $Fe_{83}B_{17}$ might be from magnetic short-range order in the $\langle S_x \rangle$ component. Short-range order will decrease the value of W and decrease the obtained estimate of $\langle S_x \rangle$. It is therefore possible that the $Fe_{80}B_{20}$ sample has more magnetic short-range order in $\langle S_x \rangle$ than the $Fe_{83}B_{17}$ sample and that the degree of canting for both samples is considerably less than predicted by the theoretical calculations of Liebs and Föhnle (1996).

Care must be taken in comparisons between the experimental results presented here and the works of Liebs and Föhnle (1996), as measuring the mass density of an amorphous ribbon is difficult and prone to error. Even so, Liebs and Föhnle have predicted that there should be no canting in 7.08 g cm^{-3} , but canting becomes stable with increasing mass density. This appears to be in contradiction with the experimental results here, where canting is observed in a sample with mass density 6.80 g cm^{-3} .

A further comparison with the previous work can be made by examining the ratios $(d\sigma^{++}/d\Omega + d\sigma^{+-}/d\Omega)/(d\sigma^{--}/d\Omega + \sigma^{-+}/d\Omega)$. As can be seen from equations (1), the only difference between the denominator and the numerator in this ratio is due to magnetic scattering from the sample. For $\text{Fe}_{80}\text{B}_{20}$, this ratio is 3.5 ± 0.4 at the position of the first maximum in the scattering (i.e. $Q = 3.1 \text{ \AA}^{-1}$). This compares very well to the value of 3.1 ± 0.1 for $\text{Fe}_{83}\text{B}_{17}$ given by Cowley *et al* (1991) for the same maximum.

Figures 4(a) and 5(a) show that the addition of ruthenium to the samples has had the opposite effect to what was expected, because each shows that the spin-flip cross-sections are significantly smaller than those of $\text{Fe}_{80}\text{B}_{20}$. There is also little or no dependence of the spin-flip scattering on the wavevector Q . Thus, canting in FeB metallic glasses is suppressed significantly, if not completely, by the presence of ruthenium.

The ratio $(d\sigma^{++}/d\Omega + d\Omega^{+-}/d\Omega)/(d\sigma^{--}/d\Omega + d\sigma^{-+}/d\Omega)$ for $Q = 3.1 \text{ \AA}^{-1}$ has also been calculated for these samples, and has the values 3.1 ± 0.4 for $\text{Fe}_{70}\text{Ru}_{10}\text{B}_{20}$ and 1.8 ± 0.2 for $\text{Fe}_{62}\text{Ru}_{18}\text{B}_{20}$. These values show that the introduction of ruthenium decreases the magnetic scattering and so there is a decrease in the total moment per magnetic atom with increasing ruthenium concentration. This is in agreement with the behaviour of the measured moment as a function of increasing ruthenium concentration (Paulose *et al* 1987).

5.2. Variation of the magnetic structure of $\text{Fe}_{62}\text{Ru}_{18}\text{B}_{20}$

The variation of the magnetic structure in the $\text{Fe}_{62}\text{Ru}_{18}\text{B}_{20}$ alloy has been studied as a function of temperature and applied field. This glass is reported to be ferromagnetic below 200 K and a spin glass below 60 K (Paulose *et al* 1988). Therefore the three measurements described in section 3 were carried out to investigate this—one measurement at 100 K; and two measurements at 4.2 K, one with the sample field cooled; and the other with it cooled in zero field.

Figures 6 and 7 show the non-spin-flip and spin-flip cross-sections from these measurements. The magnitude of the spin-flip scattering in all three diagrams of figure 6 is extremely small. In contrast the non-spin-flip scattering from the field cooled measurement is considerably larger than that from the other two measurements. This difference in the non-spin-flip scattering indicates that the magnitude of S_z depends on the history of this sample in the magnetic field.

In principle it is possible to extract the value of S_z from this data. Examination of equations (1) show that $d\sigma^{++}/d\Omega$ and $d\sigma^{--}/d\Omega$ contain both atomic and magnetic coherent scattering, as well as incoherent contributions. In addition, these cross-sections contain crossed nuclear and magnetic terms. The incoherent contributions can be calculated (Sears 1992) and the coherent nuclear scattering could be estimated using the x-ray diffraction data, but this would be subject to systematic errors. However, future measurements with the polarization parallel to the scattering vector will be possible on IN20 to measure the atomic and magnetic cross-sections directly.

Although it is difficult to extract an *absolute value* of S_z as a function of temperature and field history dependence from this data, it is nevertheless possible to determine whether there is any *variation* of S_z in the $\text{Fe}_{62}\text{Ru}_{18}\text{B}_{20}$ sample. Equations (1) show that by subtracting the sum $\frac{1}{2}(d\sigma^{++}/d\Omega + d\sigma^{--}/d\Omega)$ for the zero-field cooled measurement from the sum $\frac{1}{2}(d\sigma^{++}/d\Omega + d\sigma^{--}/d\Omega)$ for the field cooled measurement and assuming that the atomic structure of the glass remains unchanged, the incoherent and coherent nuclear cross-sections for $\text{Fe}_{62}\text{Ru}_{18}\text{B}_{20}$ will vanish, as will the terms consisting of the multiplication of magnetic and nuclear scattering lengths. The remainder is the difference between the S_z contributions for the two field history dependent measurements. Similar calculations give the difference in

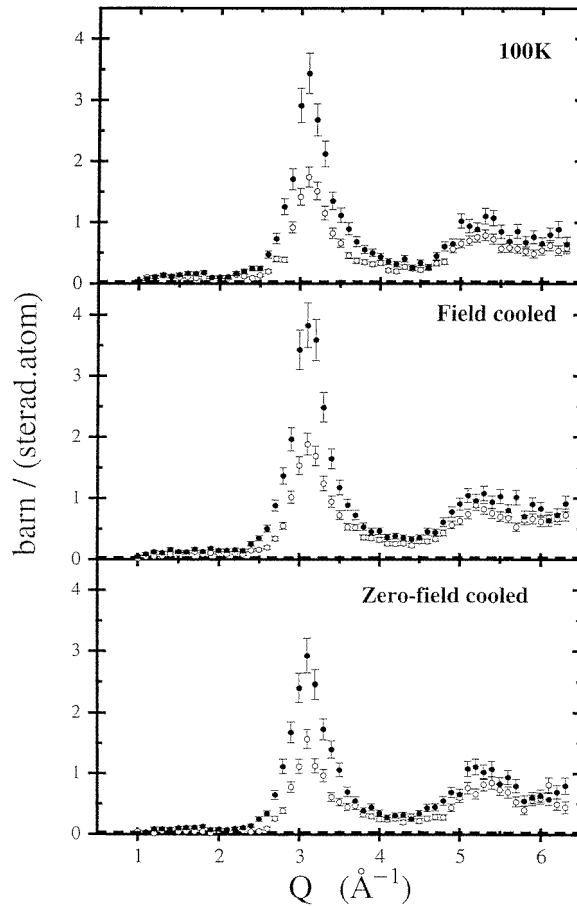


Figure 6. The non-spin-flip cross-sections from $Fe_{62}Ru_{18}B_{20}$ as a function of temperature and field history. The format and definitions are as for figure 3(b).

the magnitudes of S_z between the field cooled and 100 K measurements, and the zero-field cooled and 100 K measurements. The resultant data are shown in figure 8 and in both cases the difference in the S_z contribution is approximately zero, except for close to the value $Q = 3.1 \text{ \AA}^{-1}$ where a peak appears. This value of Q corresponds to the maximum in the non-spin-flip cross-sections. The size of the S_z contribution is largest for the field cooled experiment and smallest for the zero-field cooled experiment.

The fact that the S_z contribution at 100 K than for a field-cooled sample at 4.2 K is expected because the higher temperature will produce more fluctuations. The difference between the field cooled and zero-field cooled S_z contributions and at the same time the absence of an S_x contribution are not consistent with the presence of a spin-glass phase. If $Fe_{62}Ru_{18}B_{20}$ is a spin glass (Paulose *et al* 1986), the magnetic scattering from the zero-field cooled sample will contain information on the orientations of the frozen moments and on any magnetic short-range order that is present. This scattering will be apparent in both the spin-flip and non-spin-flip cross-sections, since for a spin glass the projections S_x and S_z will be equivalent. Figure 7 shows no structure in S_x as a function of the field history and therefore on a local scale the moments are not glassy. The fact that

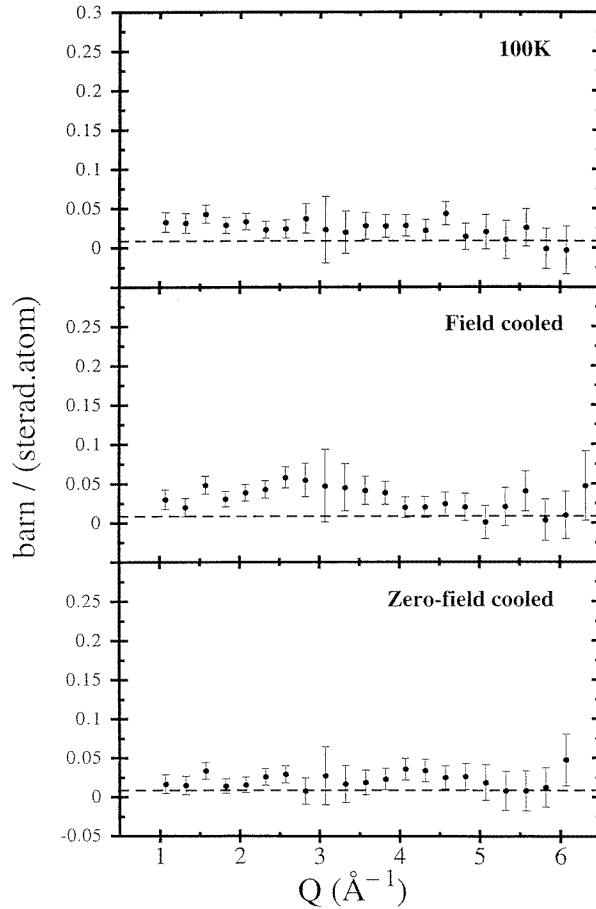


Figure 7. The spin-flip cross-sections from $\text{Fe}_{62}\text{Ru}_{18}\text{B}_{20}$ as a function of temperature and field history. The format and definitions are as figure 3(a).

there is a difference in the S_z contributions between the field cooled and zero-field cooled measurements suggests that there is a freezing in the magnetic configuration in this sample upon cooling.

A possible explanation may be that there is a small population of antiferromagnetically coupled moments, as in the models developed by Hafner *et al* (1994), which is weighted depending upon the field history of the sample. This would change the configurational average of S_z without providing a corresponding contribution to S_x .

A second explanation is this: the moments are grouped into regions sufficiently large that scattering from them occurs at smaller Q than that observed in this experiment. The local magnetization is largely collinear *within* each region, but there are spin-glass-like correlations *between* the regions. Such a model may explain both these results and the findings of Paulose *et al* (1988). The non-spin-flip scattering is sensitive to the projection of the magnetic moment along the z direction. When cooled in zero field, the moments within any given region will be collinear, but the regions themselves will be randomly aligned. Thus the configurational average of S_z will be smaller than if the sample were cooled in a field, which creates a 'preferred direction' for all the moments. In both

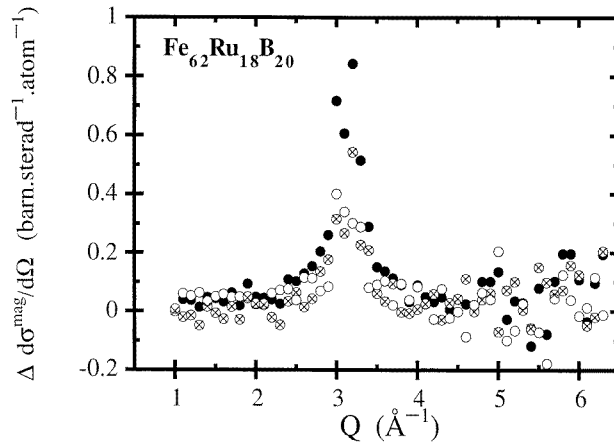


Figure 8. Difference plots of the cross-sections $\frac{1}{2}(\text{d}\sigma^{++}/\text{d}\Omega + \text{d}\sigma^{--}/\text{d}\Omega)$ are given for various pairs of measurements of $Fe_{62}Ru_{18}B_{20}$. Plotted are: field cooled – zero-field cooled (●); field cooled –100 K (⊗); and 100 K – zero-field cooled (○).

cases the configurational average of S_x is very small. Bulk measurements of the magnetic susceptibility are sensitive to the *mean* magnetic moment, however, and will detect spin-glass correlations between the regions. The formation of regions in alloys with critical concentrations close to the ferromagnetic regime has been seen in a number of other systems (e.g. Hicks *et al* 1969). Both explanations of the magnetic properties of the $Fe_{62}Ru_{18}B_{20}$ glass are consistent with the results of Paulose *et al* (1988).

Neither model necessarily implies chemical clustering of the iron atoms in these samples, which in any case has not been observed in the SAS data. These models cannot be rigorously tested in the context of either this IN20 experiment or the SAS experiments to date, as neither measurements have been designed to be sensitive to magnetic scattering at very low Q . Such scattering would contain information about the spin-glass-like correlations over a length scale of many atoms. This is required to determine whether either of the above proposed explanations is valid and such a measurement will be the focus of future work.

It should be added that if the applied magnetic field were insufficient to saturate the magnetic domains in the sample, a similar result to that reported would be observed. However, there are good reasons to believe that a magnetic field of 2 T is sufficient to saturate the domains in the sample and in addition a lack of saturation would not account for the field history dependence of the magnetic properties of $Fe_{62}Ru_{18}B_{20}$.

6. Conclusion

The ferromagnetic metallic glass $Fe_{80}B_{20}$ has been found to have significant canting of magnetic moments, with an average angle estimated to be $49 \pm 6^\circ$ to the saturating field direction. The introduction of ruthenium in $Fe_{80-x}Ru_xB_{20}$ glasses has been found to suppress that canting. $Fe_{62}Ru_{18}B_{20}$ metallic glass exhibits no measurable canting, but there is a difference in the magnetic scattering from this sample at 4.2 K depending on its field history.

Acknowledgments

The authors would like to thank the Institut Laue–Langevin for the use of the IN20 instrument. Thanks also to Mr J Newell for his assistance in sample preparation, and to Mr P Howe for his help in writing the analysis software. Our interest in these materials was stimulated by discussions with Dr P L Paulose to whom we are grateful. This work was funded by the EPSRC.

References

- Al-Heniti S and Cowlam N to be published
Bletry J and Sadoc J F 1975 *J. Phys. F: Met. Phys.* **5** L111
Brown P J 1995 *International Tables for Crystallography* vol C, ed A J C Wilson (Dordrecht: Kluwer) pp 391–9
Cowley R A, Patterson C, Cowlam N, Ivison P K, Martinez J and Cussen L D 1991 *J. Phys.: Condens. Matter* **3** 9521
Guoan Wu, Cowlam N, Davies H A, Cowley R A, Paul D McK and Stirling W 1982 *J. Physique. Coll.* **13** C7 71
Hafnet J, Tezge M and Becker C 1994 *Phys. Rev. B* **49** 285
Harders T M, Hicks T J and Wells P 1985 *J. Appl. Crystallogr.* **18** 131
Harker S J and Pollard R J 1989 *J. Phys.: Condens. Matter* **1** 8269
Hicks T J, Rainford B, Kouvel J S, Low G G and Comly J B 1969 *Phys. Rev. Lett.* **22** 531
Kaul S N and Babu P D 1994 *Phys. Rev. B* **50** 9308
Krompiewski S, Krauss U and Krey U 1989 *Physica B* **161** 219
Liebs M and Fähnle M 1996 *J. Phys.: Condens. Matter* **8** 3207
Lovesey S W 1984 *Theory of Neutron Scattering from Condensed Matter* vol 2 (Oxford: Clarendon)
Moon R M, Riste T and Koechler W C 1969 *Phys. Rev.* **181** 920
Paulose P L, Nagarajan R, Nagarajan V and Vijayaraghavan R 1986 *J. Magn. Magn. Mater.* **54–57** 257
———1987 *Solid State Commun.* **61** 151
———1988 *Solid State Commun.* **67** 685
Sears V F 1975 *Adv. Phys.* **24** 1
———1992 *Neutron News* **3** 26